FUSION OF HYPERSPECTRAL AND MULTISPECTRAL IMAGES USING NON – SUBSAMPLED CONTOURLET TRANSFORM

S.Jeyaanusuya, Associate professor, ECE department, jeyaanusuya@yahoo.com
1.B.Sharmilaa,ECE department,balakrishnansharmila@gmail.com
2.R.Vaishali, ECE department, vaishalimala1973@gmail.com
3.S.Vinusha, ECE department, reply2vinusha@gmail.com

ABSTRACT

Unlike multispectral (MSI) and panchromatic (PAN) images, generally the spatial resolution of hyperspectral images (HSI) is limited, due to sensor limitations. In many application HIS with a high spectral as well as spatial resolutions are required. In this paper' a new method for spatial resolution enhancement of a HSI using spectral unmixing and sparse coding (SUSC) is introduced. The proposed method fuses high spectral resolution features from the HSI with high spatial resolution features from an MSI of the same scene.Endmembers are extracted from the HSI by spectral unmixing, and the exact location of the endmembers is obtained fom the MSI. This fusion process by using spectral unmixing is formulated as an ill-posed inverse problem which requires the regularization term in order to convert it into a well-posed inverse problem. As aregularizer, we employ sparse coding (SC), for which a dictionary is constructed using high spatial resolution MSI or PAN images from unrelated scenes. The proposed algorithm is applied to real hyperion and ROSIS data sets. Sharpening,spectral unmixing and SC methods, the proposed method is shown to significantly increase the spatial resolution while preserving the spectral content of the HSI.

Index terms-Fusion, Hyperspectral images (HIS), Multispectral (MSI), sparse coding(SC),spectral unmixing.

I.INTRODUCTION

Remote sensing images have been widely used in different practical applications such as agriculture, forestmonitoring environmental studies, and military application [1}.The main types of remote sensing images are Panchromatic (PAN), Multispectral (MSI), and Hperspectral images (HSI). PAN images have a high spatial resolution and spatial structures are well defined,but they are limited to one gray – scale image band.MSI have low spatial resolution than PAN images and contain a limited number of spectral bands. HIS usually have lower spatial resolution than MSI and PAN images but have a high spatial resolution [2].

HSI have been used in many different practical applications. In various applications, HSI spectral and spatial resolutions are required [2].

In this paper, a new method for spatial resolution enhancement of HIS is proposed, based on the fusion of HSI and MSI using the LMM. In the proposed method, the HRHSI reconstruction problem is formulated as a linear inverse problem (LIP). An LIP is generally ill- posted and does not have a unique solution. A regularization term needs to be included to convert it into a well-posed inverse problem. In the proposed method, the regularization term is constructed based on SC, for which dictionary is constructed by several high spatial resolution MSI or PAN images which are unrelated to the HSI. In this way, a method is obtained, which simultaneously makes use of the LMM to avoid spectral distortion and SC to optimize the spatial resolution improvement.

The proposed spectral unmixing and SC (SCSU) algorithm is applied to real datasets and

compared with state-of-the-art algorithms using pansharpening [6],[7],[23], SC [13], LSU [20], and CNMF [21]. The results obtained by SUSC or superior to these methods from the state of the art.

II. PROPOSED METHOD

We assume that a HSI and an MSI or PAN image of the same scene are available. As a first step, before the introduction of proposed method, preprocessing is performed to reduce the noise in the HSI. For this, we apply a recently a proposed method, presented in [24]. Then, LMM is applied. In this model, the endmembersare extracted using the spectral properties of the low-resolution HSI (LRHSI,which is observed HSI).After that the initial abundance fractions are calculated using the spatial properties from the MSI. From this, an initial estimate of the HRHSI is obtained. The proposed fusion method then iteratively updates the abundance fractions. At the end, the spectral of each HRHSI pixel is reconstructed based on the LRHSI endmembers.

The fusion process of the HSI and MSI is formulated as an ill-posed inverse problem. A regularization term is used to convert it into a well-posed inverse problem. The regularization term is constructed based on SC. We construct a proper dictionary with several high spatial MSI or PAN images from unrelated scenes. Based on this dictionary and the initial HRHSI obtained from LMM, the SC is estimated. By using the SC as the regularization term, the abundance fractions are calculated by solving the well-posed inverse problem. The final HRHSI is obtained from the obtained abundance fractions and the endmembers. In the following, we will explain the different steps of the procedure in more detail.

III. NSCT DECOMPOSITION

NSCT decomposition is to compute the multi scale and different direction components of the discrete images. It involves the two stages such as non-sub sampled pyramid(NSP) and non-sub sampled directional filter bank(NSDFB) to extract the texture, contours and detailed coefficients. NSP decomposes the image into low and high frequency subbands at each decomposition level and it produces n+1 sub images if decomposition level is n.NSDFB extracts the detailed coefficients from direction decomposition of high frequency subbands obtained from NSP. It generates m power of 2 direction sub images if number of stages be m.

IV. UP SAMPLING

It is a method of constructing new data points within the range of a discrete set of known data points. It increases the samples of each multi spectral bands twice at frequency domain to make better fusion process. Here, upsampling will be done using Bicubic interpolation method. It is an extension of cubic interpolation for interpolating data points on a two dimensional regular grid.Bicubic interpolation can be accomplished using either Lagrange polynomials, cubic splines, or cubic convolution algorithm.

V. IMAGE FUSION

The high frequency subbands of two source images obtained from NSCT are utilized for morphing process to get the enhanced information. Here, the pixel level fusion method is approached for this process. It will be implemented based on maximum rule and energy measurement for coefficient selection.At fusion stage, The low frequency subband of multi spectral image remain unchanged and high frequency subbands will be fused by energy and WAMM to select desired coefficients.Finally, fused frequency subbands are inverse

transformed to reconstruct the fused image and *parameters will be evaluated between input and* fused image.

Continues……

PSNR (Peak Signal to Noise Ratio)

PSNR = 10 *log 10 255/MSE*

RMSE (Root Mean Square Error)

*MSE = (1/M*N)* $\sum\sum$ *(*a_{ij} –b_{ij}*)^2*

RMSE = sqrt (MSE)

Where,

M,N are Number of Rows and Columns

a_{ij} – Original Image and b_{ij} – Fused Image

Continues..

Correlation Coefficient: It is used to find the similarity between two different images with their intensities. It will be described by,

Cor_coef = ***[sum(sum(u1.*u2))] /***

[sqrt(sum(sum(u1.*u1))*sum(sum(u2.*u2)))];

Where, u1 = a_{ij} – mean of a_{ij}, u2 = b_{ij} – mean of b_{ij}.

Percentage Residual Difference(PRD): It is used to measure the difference between original Image and Restored Image.

PRD = sqrt(sum((F1 – F2).^2)/sum(F1))

Where, F1 – Original Image and F2 – Fused Image.

VI. OBSERVATION MODEL

Let us first define the observation models. In general, HSI and MSI have three dimensions, two spatial dimensions, and one spectral. For notational convenience, these images are converted to two dimensions [12]. If we define Z as the HRHSI (desired image), Yh as the low spatial resolution HSI (LRHSI), and Ym as the MSI from the same scene, their relationship can be expressed as [21]

Yh= ZBM + Nh; Z∈R Lh×nm,B∈R nm×nm,

M∈R nm×nh,Y h ∈R Lh×nh,N H ∈R Lh×nh (1)

Ym = RZ + Nm; Ym∈R Lm×nm,

R∈R Lm ×Lh ,Nm∈nm.

(2) Equation (1) models the relationship between the HRHSI Z (with Lh bands and nm pixels) and the LRHSI Yh.

VII. OPTIMIZATION PROBLEM

The fusion of the HSI and the MSI is formulated as an LIP

argmin X 1/ 2 Yh−EXBM2 F + λm 2Ym−REX2 F+λ 2ϕ(x)…….. (6)

where ϕ(x) is a regularization term. The inverse problem of (6) can be ill-posed or well posed, depending on the reduced dimension of the images and the number of spectral bands [28]. If the product of the matrices R and E has a full column rank, the LIP problem is well posed. However, if there are fewer bands in the MSI than the number of endmembers, the matrix (RE) cannot have full column rank, which turns the LIP prob- lem in an ill-posed one. In this paper, (6) is assumed to be an ill-posed LIP. Therefore, a regularization term is required. The first two terms are the fidelity terms, describing that the esti- mated image is able to explain the observed data according to the models defined in (4) and (5). The last term is the regular- izer. The parametersλm and λ control the relative importance of the various terms [12].

VIII. SPECTRAL UNMIXING MODEL AND DIMENSION REDUCTION

The first step is the use of the LMM Z = EX + N.. (3)

where E ∈RLh×P (P represents the number of endmembers) is the endmember signature matrix that can be, e.g.,extracted by vertex component analysis (VCA) [25] or N- FINDR [26],

X ∈R P×nm is the abundance fraction matrix,

and N ∈R Lh×nm represents the noise matrix. By substituting (3) into the observation models defined by (1) and (2), we have approximatelyYh ≈ EXh,Xh = XBM (4) Ym ≈ EmX,Em = RE. (5) According to (3), the construction of Z requires the endmembers and abundance fractions.

From (4), we deduce that the HRHSI has the same endmembers as the HSI, and the abundance fractions of the HSI are obtained from the spatially degraded abundance fractions of the HRHSI. Therefore, the required endmembers can be extracted from the original HSI. A supe r resolution method then only requires the determination of the abundance fractions. An initial estimate of these fractions is obtained from the MSI by using (5). In this work, we use the variable splitting and augmented (SUNSAL) algorithm [27] to do so. That the endmembers can be directly obtained from the HSI, not only means a reduction in the computational load, but the final HRHSI is also expected to have low spectral distortion.The first step is the use of the LMM,

Z = EX + N (3) where E ∈RLh×P (P represents the number of endmem- bers) is the endmember signature matrix that can be, e.g.,

extracted by vertex component analysis (VCA) [25] or N- FINDR [26], X ∈

R P×nm is the abundance fraction matrix,

and N ∈R Lh×nm represents the noise matrix.

By substituting (3) into the observation models defined by (1) and (2), we have approximately Yh ≈ EXh,Xh = XBM (4) Ym ≈ EmX,Em = RE. (5) According to (3), the construction of Z requires the endmembers and abundance fractions.

From (4), we deduce that the HRHSI has the same endmembers as the HSI, and the abundance fractions of the HSI are obtained from the spatially degraded abundance fractions of the HRHSI. Therefore, the required endmembers can be extracted from the original HSI. A super resolution method then only requires the determination of the abundance fractions. An initial estimate of these fractions is obtained from the MSI by using (5).

In this work, we use the variable splitting and augmented (SUNSAL) algorithm [27] to do so. That the endmembers can be directly obtained from the HSI, not only means a reduction in the computational load, but the final HRHSI is also expected to have low spectral distortion.

IX. SPARSE CODING

Although image content can vary greatly from image to image, the microstructures of images can be represented by a small number of structural primitives (e.g., edges, line segments, and other elementary features). These microstructures are the same for all images [2]. SC relies on this observation by constructing a dictionary of such primitives from a number of images and uses this dictionary to reconstruct a specific image from the smallest number of dictionary atoms. In the proposed method, we use the concept of SC for the regularization. A dictionary (φ) is constructed with microstructures of unrelated MSI or PAN images of high spatial resolution. Then, a sparse code (S) for the HRHSI is calculated from the smallest number of dictionary atoms, where each

pixel is represented by a linear combination of a few atoms. The optimization problem becomes

argmin X,S 1/ 2 Yh −EXBM2 F+λm 2 Ym −REX2 F +λ 2 φS −EX2 F ….. (7)

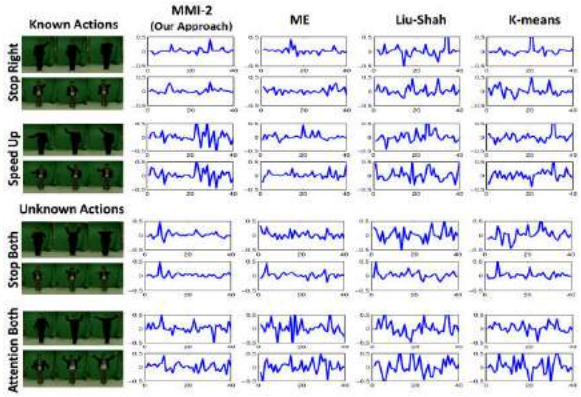

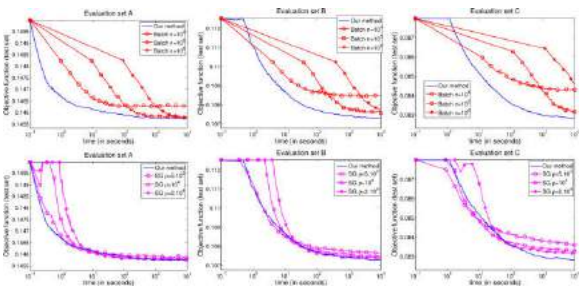

Usually, to generate the dictionary, the images are divided into several patches. Also, in order to construct the image with this dictionary, it is divided into several patches which are separately reconstructed by the dictionary atoms. In recent lit- erature, overcomplete dictionaries with dimensions larger than the image dimensions have been considered. Different methods such as online dictionary learning (ODL) [29] and K-means singular value decomposition (K-SVD) [30] have been devel- oped for constructing an overcomplete dictionary. There is no unique rule to select the dictionary size and the number of atoms. Generally, the smaller the patches, the more atoms can be determined. However, too small patches are not efficient to properly capture the textures, edges, etc. With larger patch sizes, a larger number of atoms are required to guarantee the overcompleteness (which requires a larger computational cost). In general, the size of the patches is empirically selected [28]. In the proposed method, the dictionary was produced by the K- SVD algorithm, trained on a dataset of 10 000 patches with size 8×8. Those patches are taken from an arbitrary set of natural images (unrelated to the test images). In fact, the res- olution of these images should be sufficiently high to capture the image details. As an example, MSI from the advanced land imager (ALI) sensor . The con-structed dictionary by using the K-SVD algorithm is shown .

After constructing the proper dictionary, the HRHSI can be obtained from a linear combination of a small number of atoms from the dictionary. The matrix with the obtained coefficients is called the sparse code [31]. It is obtained by ˆ

S argmin S 1/2 Z initial −φSSubject toS0 ≤ K…… (8)

where K is the number of atoms needed for reconstructing Z initial patches. Z initial can be estimated by interpolation [16], but in the proposed method, it is obtained from (3). For intro- ducing sufficient sparsity, K is chosen much smaller than the number of dictionary atoms. In this paper, the sparse code is estimated by orthogonal matching pursuit (OMP) [32].

X. COMPLEXITY ANALYSIS

The SALSA algorithm has a complexity of O1(Pnitnmlog(Pnm)), where nit is the number of SALSA iterations, P is the number of endmembers, and nm is the total number of pixels [28], [34]. The computational com-plexity of the SC is O2(KnpLh), where K is the number of dictionary atoms and np is the patch size. Therefore, the complexity of the proposed algorithm is Nth(O1(Pnitnmlog(Pnm)) + O2(KnpLh)), where Nth is max_iteration.

XI.PANSHAEPENING METHODS

: For the spatial resolution enhancement of HSI, the Gramm–Schmidt (GS) procedure of [6], the adaptive GS (GSA) method of [7], the smooth-ing filter-based intensity modulation method (SFIM) of [23], and a modulation transfer function generalized Laplacian pyramid with high-pass modulation (MTF_GLP_HPM) from [41] are applied to the first dataset along with the proposed SUSC method. All the methods are implemented in Matlab on a computer with an Intel(R) Core(TM) i5-3210 processor (3.1 GHz), 4 GB of memory, and a 64-bit Operating System. Fig. 3 shows the obtained results for one specific subimage.

wavelength (0.4–0.9 μm). The simulation results show that in CS-based fusion techniques (GS, GSA), the spatial resolution of the reconstructed image is low and the spectral distortion is high because of the spectral mismatch between the PAN image and the HSI spectral range. In the MRA approaches (SFIM, MTF_GLP_HPM), the spatial resolution is low but the spectral distortion is lower than with the CS methods. The reconstructed images by the proposed method SUSC are visually very close to the ground truth images. As is shown in Table I, the spectral distortion is the lowest in the proposed method. The required computing time of the proposed method, however, is much higher than the pansharpening methods.

The construction of the dictionary and the estimation of the sparse code take aconsiderable amount of time. Moreover, the method iteratively updates the abundance fractions and the sparse code, which makes the proposed method time consuming. 2) SUSC Methods: The SC method from [13], CNMF from [21], and LSU from [20] are applied to the second dataset. In CNMF, the maximum number of iterations in the inner and outer loops is selected as 10 and 300, respectively. In LSU, the image is divided into several patches, and the proper size for the patches is related to the number of endmembers in each patch. In the experiment, different patch sizes were applied. Using SUSC, the same parameters as in the first dataset are applied. Quality measures and computing time for the proposed algorithm and the other algorithms are reported in Table II. Fig. 4 shows results for band 170 of a specific subimage.

The simulation results show that SC produces high spatial resolution HRHSI because of the use of the high spatial resolution dic- tionary, but spectral distortion occurs. Using LSU and CNMF, the spectral distortion is lower than for SC, but the spatial resolution is limited. The reconstructed image by the proposed method is visually very close to the ground truth image. The PSNR, ERGAS, and CC in function of the wavelength (0.4–2.5 μm) are shown in Figs. 8–10, respectively. Fig. 11 shows the spectra of pixel (1100) in the ground truth and reconstructed image; the spectral distortion value is lowest in the proposed method. In the proposed method, spectral unmixing is used to preserve the spectral content of the HSI, and SC is used to enhance the spatial resolution of the HSI. Therefore, the reconstructed HRHSI have, simultaneously, a higher spatial and spectral resolutions compared to the other methods.

XII. DATA SET

The proposed method has been applied to two real datasets. The first dataset was acquired by the reflective optics system imaging spectrometer (ROSIS) optical sensor over the

This article has been accepted for inclusion in a future issue of this journal. Content is final as presented, with the exception of pagination.urban area of the University of Pavia, Italy.1 The image size is 610×610×103 with a spatial resolution of 1.3 m. For these HSI, a MSI of the same scene does not exist. Therefore, we

generate an MSI of four band by filtering the HSI with the IKONOS-like reflectance spectral responses. With these, R andB are estimated as in [12]. In fact, the IKONOS satellite captures both a PAN (0.45–0.90 μm) and four multispectral bands (0.45–0.52, 0.52–0.60, 0.63–0.69, and 0.76–0.90 μm). On the HSI, the water vapor absorption bands are removed. The obtained HSI is applied as the ground truth image with high spatial and spectral resolutions. For constructing an LRHSI, Gaussian blurring (B) (with dimension 7×7 and σ =1 .5) is applied to the ground truth images and the blurred images are downsampled by a factor of 4 (M). For the simulations, ground truth subimages are selected with size 120×120×93 leading to LRHSI with size 30×30×93 and MSI with size 120× 120×4. For the dictionary, twenty PAN QuickBird images2 with a spatial resolution 0.7 m, which are unrelated and do not overlap with the test images, have been used. These images are downsampled by a mean filter with a factor of 2 in order to have the same spatial resolution as the HRHSI. Fig. 3 shows for one of the subimages band 10 of the ground truth image and the LRHSI, band 2 of the MSI, and the PAN image. SUSC is applied to these images, and the reconstructed HRHSI is compared with the ground truth images. The second dataset contains images taken above Shiraz city in Iran, and was obtained by two instruments, the Hyperion instrument, and the ALI.3 Hyperion is a hyperspectral imager with a spatial resolution of 30 m, the entity ID of the Hyperion image is EO1H1630392004316110PV_1R1. It has size 3858×256×242.

The ALI instrument provides MSI and PAN of the same scene at resolutions of 30 and 10 m, respectively. The MSI are used in our experiment. The entity ID of the ALI data is EO1A1630392004316110PV_1GST. It has size 4241×256×10. First the HSI and MSI are geometrically coregistered. Then, the water absorption bands (1–7, 58–76, 121–128, 165–180, 221–242) are removed from the HSI, and it is denoised using [24]. A LRHSI is constructed from it in the same way as described for the first dataset. Also, since the original HSI and MSI of this dataset have the same resolution, we set B = I and estimate R. In the simulations, ground truth images are selected with size 120×120×170, and LRHSI with size 30×30×170 and MSI with size 120×120×9 are obtained. Fig. 4 shows for one of the subimages band 170 of the ground truth image and the LRHSI and band 2 of the MSI.

The proposed algorithm is applied to these images, and the reconstructed HRHSI are compared with the ground truth images. In the proposed method, VCA is used for endmemberextrac- tion. Since VCA is not robust, we performed ten runs of the algorithm and report the average of the corresponding results. The number of endmembers is equal to the number of MSI bands. For constructing the dictionary, the PAN images are converted to 10 000 patches with size of (8×8). Then 40 atoms of the dictionary are used for constructing the HRHSI..

solving the optimization problem, the regularization parameters are selected as: λm =1and μ =5×10−2 for both datasets [12], [28]. In order to select an appropriate value of λ, the per-formance of the proposed algorithm has been evaluated as a function of λ. Figs. 5 and 6 display the results for the first and second datasets, respectively. The optimal value of λ is found to be one.

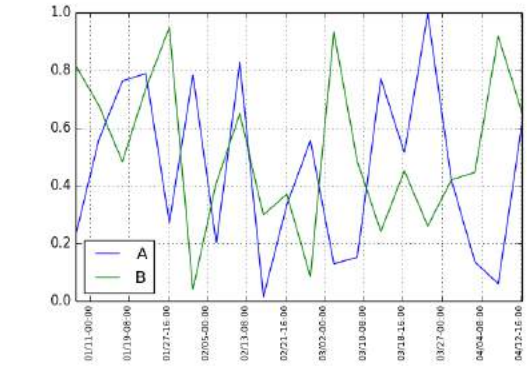

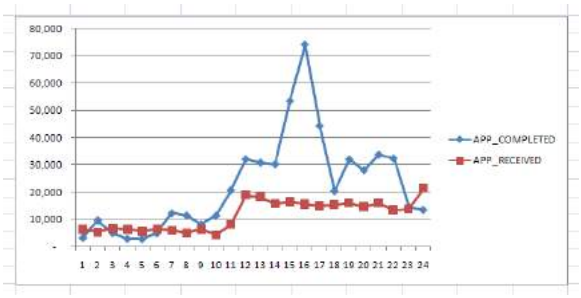

For image- based applications, such as still pictures, stream video, voice, animal sounds and monitoring data, one uses a wireless sensor networkwhereby the nodes arecamera-equipped[2].

XIII. COMPARISON WITH OTHER FUSION METHODS

The proposed method is compared with state – of-the-art algorithms. considerable amount of time. Moreover, the method iteratively updates the abundance fractions and the sparse code, which makes the proposed method time consuming. 2) SUSC Methods: The SC method from [13], CNMF from [21], and LSU from [20] are applied to the second dataset. In CNMF, the maximum number of iterations in the inner and outer loops is selected as 10 and 300, respectively. In LSU, the image is divided into several patches, and the proper size for the patches is related to the number of endmembers in each patch. In the experiment, different patch sizes were applied. Using SUSC, the same parameters as in the first dataset are applied. Quality measures and computing time for the proposed algorithm and the other algorithms are reported in Table II. Fig. 4 shows results for band 170 of a specific subimage. The simulation results show that SC produces high spatial resolution HRHSI because of the use of the high spatial resolution dic- tionary, but spectral distortion occurs. Using LSU and CNMF, the spectral distortion is lower than for SC, but the spatial res- olution is limited. The reconstructed image by the proposed method is visually very close to the ground truth image. The PSNR, ERGAS, and CC in function of the wavelength (0.4–2.5 μm) are shown in Figs. 8–10, respectively. Fig. 11 shows the spectra of pixel (1100) in the ground truth and reconstructed image; the spectral distortion value is lowest in the proposed method. In the proposed method, spectral unmixing is used to preserve the spectral content of the HSI, and SC is used to enhance the spatial resolution of the HSI. Therefore, the reconstructed HRHSI have, simultaneously, a higher spatial and spectral resolutions compared to the other methods.

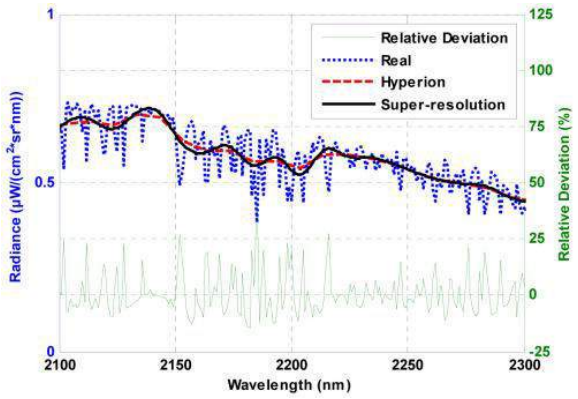

XV. CONCLUSION

In this paper, a new method for enhancing the spatial resolution of HSI based on fusion with MSI is proposed. The method combines the spectral mixing model to reduce spec- tral distortions with SC to inject high spatial information from a dictionary of unrelated high spatial resolution images. The problem is expressed as an LIP with the SC as regularizer. The inverse problem is solved by iteratively updating the abundance fractions using SALSA and the sparse code using OMP. Based on the visual and quantitative results, in the proposed method, the spatial resolution is significantly enhanced and the spectral distortion of the reconstructed image is low compared to state of the art reconstruction techniques based on local unmixing and SC. In the future, our aim is to reduce the computational complexity of the proposed algorithm.

ACKNOWLEDGMENT

The authors would like to thank Prof. J. Bioucas-Dias from the Instituto de Telecomunicaes and Instituto Superior Tcnico, Universidade de Lisboa for sharing the IKONOS-like reflectance spectral responses used in the experiments.

REFERENCES

[1] Y. Gu, Y. Zhang, and J. Zhang, "Integration of spatial–spectral information for resolution enhancement in hyperspectral images," IEEE Trans. Geosci. Remote Sens., vol. 46, no. 5, pp. 1347–1358, May 2008.

[2] Y. Zhao, J. Yang, Q. Zhang, L. Song, Y. Cheng, and Q. Pan, "Hyperspectral imagery super-resolution by sparse representation and spectral regularization," EURASIP J. Adv. Signal Process., vol. 2011, no. 1, pp. 1–10, Oct. 2011.

[3] T. Akgun, Y. Altunbasak, and R. M. Mersereau, "Super-resolution recon- struction of hyperspectral images," IEEE Trans. Image Process., vol. 14, no. 11, pp. 1860–1875, Nov. 2005.

[4] L. Loncan et al., "Hyperspectralpansharpening: A review," IEEE Geosci. Remote Sens. Mag., vol. 3, no. 3, pp. 27–46, Sep. 2015.

[5] P. Chavez, C. Sides, and A. Anderson, "Comparison of three different methods to merge multiresolution and multispectral data-LANDSAT TM and SPOT panchromatic," Photogramm. Eng. Remote Sens., vol. 57, no. 3, pp. 295–303, Mar. 1991.

[6] C. A. Laben and B. V. Brower, "Process for enhancing the spatial reso- lution of multispectral imagery using pan-sharpening," U.S. Patent US 6 011 875, 2000.

[7] B. Aiazzi, S. Baronti, and M. Selva, "Improving component substitu-tionpansharpening through multivariate regression of MS+ Pan data," IEEE Trans. Geosci. Remote Sens., vol. 45, no. 10, pp. 3230–3039, Oct. 2007.

[8] S. G. Mallat, "A theory for multiresolution signal decomposition: The wavelet representation," IEEE Trans. Pattern Anal. Mach. Intell., vol. 11, no. 7, pp. 674–693, Jul. 1989.

[9] P. J. Burt and E. H. Adelson, "The Laplacian pyramid as a compact image code," IEEE Trans. Commun., vol. TC-31, no. 4, pp. 5320–5540, Apr. 1983.

[10] J.-L. Starck, J. Fadili, and F. Murtagh, "The undecimated wavelet decom- position and its reconstruction," IEEE Trans. Image Process., vol. 16, no. 2, pp. 297–309, Feb. 2007.

[11] M. N. Do and M. Vetterli, "The contourlet transform: An efficient directional multiresolution image representation," IEEE

Trans. Image Process., vol. 14, no. 12, pp. 2091–2106, Dec. 2005.

[12] M. Simões, J. Bioucas-Dias, L. B. Almeida, and J. Chanussot, "A con- vex formulation for hyperspectral image superresolution via subspace- based regularization," IEEE Trans. Geosci. Remote Sens., vol. 53, no. 6, pp. 3373–3388, Jun. 2015.

[13] N. Akhtar, F. Shafait, and A. Mian, "Sparse spatio-spectral representa- tion for hyperspectral image super-resolution," in Proc. Comput. Vision (ECCV'14), 2014, pp. 63–78.

[14] C. Grohnfeldt, X. X. Zhu, and R. Bamler, "Jointly sparse fusion of hyper- spectral and multispectral imagery," in Proc. IEEE Int. Geosci.Remote Sens. Symp. (IGARSS), 2013, pp. 4090–4093.

[15] C. Grohnfeldt and X. X. Zhu, "Towards a combined sparse representa- tion and unmixing based hybrid hyperspectral resolution enhancement method," in Proc. IEEE Int. Geosci.Remote Sens. Symp. (IGARSS), 2015, pp. 2872–2875.

[16] M. Simes, J. Bioucas-Dias, L. B. Almeida, and J. Chanussot, "Hyperspectral imagery super-resolution by spatial joint nonlocal sim- ilarity," IEEE J. Sel. Topics Appl. Earth Observ. Remote Sens., vol. 7, no. 6, pp. 2671–2679, Jun. 2014

[17] Y. Zhao, J. Yang, and J. C.-W. Chan, "Hyperspectral image resolution enhancement based on spectral unmixing and information fusion," in Proc. Int. Arch. Photogramm. Remote Sens. Spatial Inf. Sci. (ISPRS), Hannover, Germany, 2011, pp. 33–36.

[18] M. A. Bendoumi, M. He, and S. Mei, "Hyperspectral image resolution enhancement using high-resolution multispectral image based on spectral unmixing," IEEE Trans. Geosci. Remote Sens., vol. 52, no. 10, pp. 6574– 6583, Oct. 2014.

[19] N. Keshava and J. F. Mustard, "Spectral unmixing," IEEE Signal Process. Mag., vol. 19, no. 1, pp. 44–57, Jan. 2002.

[20] G. Licciardi, M. A. Veganzones, M. Simoes, J. M. Bioucas-Dias, and J. Chanussot, "Super-resolution of hyperspectral images using local spec- tralunmixing," in Proc. Workshop Hyperspectral Image Signal Process. Evol. Remote Sens. (WHISPERS), 2014, pp. 1–4.

[21] N. Yokoya, T. Yairi, and A. Iwasaki, "Coupled nonnegative matrix factor- izationunmixing for hyperspectral and multispectral data fusion," IEEE Trans. Geosci. Remote Sens., vol. 50, no. 2, pp. 528–537, Feb. 2012.

[22] X. Liu, W. Xia, B. Wang, and L. Zhang, "An approach based on con- strained nonnegative matrix factorization to unmixhyperspectral data," IEEE Trans. Geosci. Remote Sens., vol. 49, no. 2, pp. 757–772, Feb. 2011.

[23] J. Liu, "Smoothing filter-based intensity modulation: A spectral preserve image fusion technique for improving spatial details," Int. J. Remote Sens., vol. 21, no. 18, pp. 3461–3472, 2000.

[24] A. Karami, R. Heylen, and P. Scheunders, "Hyperspectral image noise reduction and its effect on spectral unmixing," in Proc. Workshop Hyperspectral Image Signal Process.Evol. Remote Sens. (WHISPERS), 2014, pp. 1–4.

[25] J. M. Nascimento and J. M. B. Dias, "Vertex component analysis: A fast algorithm to unmixhyperspectral data," IEEE Trans. Geosci. Remote Sens., vol. 43, no. 4, pp. 898–910, Apr. 2005.

[26] M. E. Winter, "N-FINDR: An algorithm for fast autonomous spectral end-member determination in hyperspectral data," Proc. SPIE, vol. 3753, pp. 266–275, Jul. 1999.

[27] J. M. Bioucas-Dias and M. A. Figueiredo, "Alternating direction algo- rithms for constrained sparse regression: Application to hyperspectralunmixing," in Proc. Workshop Hyperspectral Image Signal Process. Evol. Remote Sens. (WHISPERS), 2010, pp. 1–4.

[28] Q. Wei, J. Bioucas-Dias, N. Dobigeon, and J.-Y.Tourneret, "Hyperspectral and multispectral image fusion based on a sparse representation," IEEE Trans. Geosci. Remote Sens., vol. 53, no. 7, pp. 3658–3668, Jul. 2015.

[29] J. Mairal, F. Bach, J. Ponce, and G. Sapiro, "Online dictionary learning for sparse coding," in Proc. 26th Annu. ICML, Montreal, QC, Canada, 2009, pp. 689–696.

[30] M. Aharon, M. Elad, and A. Bruckstein, "The K-SVD: An algorithm for designing overcomplete dictionaries for sparse representation," IEEE Trans. Signal Process., vol. 54, no. 11, pp. 4311–4322, Nov. 2006.

[31] A. S. Charles, B. Olshausen, and C. Rozell, "Learning sparse codes for hyperspectral imagery," IEEE J. Sel. Topics Signal Process., vol. 5, no. 5, pp. 963–978, Sep. 2011.

[32] R. Rubinstein, M. Zibulevsky, and M. Elad, "Efficient implementation of the K-SVD algorithm using batch orthogonal matching pursuit," CS Technion, vol. 40, no. 8, pp. 1–15, 2008.

[33] M. V. Afonso, J. M. Bioucas-Dias, and M. A. Figueiredo, "Fast image recovery using variable splitting and constrained optimization," IEEE Trans. Image Process., vol. 19, no. 9, pp. 2345–2356, Sep. 2010.

[34] M. V. Afonso, J. M. Bioucas-Dias, and M. A. Figueiredo, "An aug- mentedlagrangian approach to the constrained optimization formulation of imaging inverse problems," IEEE Trans. Image Process., vol. 20, no. 3, pp. 681–695, Mar. 2011.

[35] L. Miao and H. Qi, "Endmember extraction from highly mixed data using minimum volume constrained nonnegative matrix factorization," IEEE Trans. Geosci. Remote Sens., vol. 45, no. 3, pp. 765–777, Mar. 2007.

[36] J. Li and J. M. Bioucas-Dias, "Minimum volume simplex analysis: A fast algorithm to unmixhyperspectral data," in Proc. IEEE Int. Conf. Geosci. Remote Sens. (IGARSS), 2008, vol. 3, pp. 250–253.

[37] T.-H. Chan, C.-Y.Chi, Y.-M.Huang, and W.-K. Ma, "A convex analysis- based minimum-volume enclosing simplex algorithm for hyperspectralunmixing," IEEE Trans. Signal Process., vol. 57, no. 11, pp. 4418–4432, Nov. 2009.

[38] J. M. Bioucas-Dias, "A variable splitting augmented Lagrangian approach to linear spectral unmixing," in Proc. IEEE GRSS Workshop Hyperspectral Image SIgnal Process. Evol. Remote Sens. (WHISPERS), 2009, pp. 1–4.

[39] J. M. Bioucas-Dias and J. M. Nascimento, "Hyperspectral subspace iden- tification," IEEE Trans. Geosci. Remote Sens., vol. 46, no. 8, pp. 2435– 2445, Aug. 2008.

[40] L. Wald, "Quality of high resolution synthesised images: Is there a simple criterion?" in Proc. Int. Conf. Fusion Earth Data, Jan. 2000, pp. 99–105.

[41] G. Vivone, R. Restaino, M. Dalla Mura, G. Licciardi, and J. Chanussot, "Contrast and error-based fusion schemes for multispectral image

pan- sharpening," IEEE Geosci. Remote Sens. Lett., vol. 11, no. 5, pp. 930– 934, May 2014.